LHCb VELO Bandgap Temperature Calibration

Henar Parro Alonso
Supervisors: Edgar Lemos Cid & Victor Coco

September 2023

Abstract

This report presents the Summer Student Program project focused on the calibration method for temperature measurement of each ASIC within the VErtex LOcator, a sub-detector of the LHCb experiment at CERN. Using the WinCC Open Architecture tool, a control panel is designed to display calibrated temperature data along with raw temperature and voltage readings in real-time. This panel enhances error identification and provides more precise experiment control when operating at power levels different from the operational state.

Contents

1 Introduction

The Large Hadron Collider beauty (LHCb) experiment specializes in exploring subtle distinctions between matter and antimatter by studying a particular particle known as the "beauty quark", "bottom quark" or "b quark." In contrast to other experiments that enclose the entire collision point with a sealed detector, the LHCb experiment employs a series of subdetectors primarily to detect forward moving particles, those propelled by the collision in one direction. The first subdetector is positioned close to the collision point, with subsequent subdetectors arranged one after the other along a 20 meter length. The LHC generates a variety of quark types that swiftly decay into other forms. To capture the b quarks, LHCb has developed sophisticated movable tracking detectors situated close to the path of the beams circulating within the LHC.

The VErtex LOcator (VELO) is the first positioned detector that surrounds the interaction region at LHCb. Its principal task is to enable LHCb to trigger on and reconstruct displaced vertices, as well as playing a significant role in the tracking. The detector consists of 52 modules, each equipped with four silicon pixel sensors capable of 40 MHz readout. Each sensor is readout by three VeloPix ASICs, mounted in a module known as tile. Therefore, each module is composed of 12 ASICs. The arrangement of the modules is such that they surround the beam pipe, with the two halves of each module facing each other.

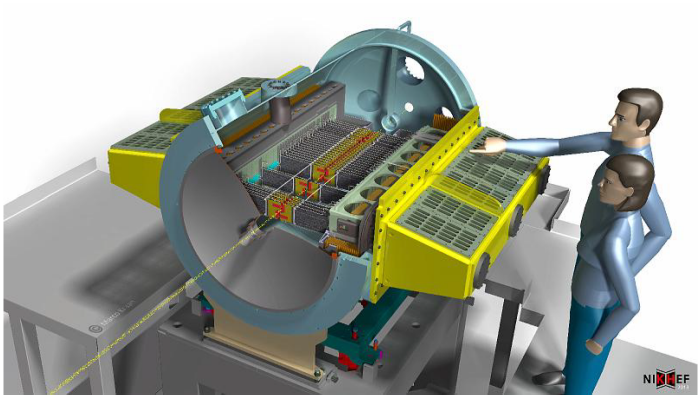

Figure 1: Artist's impression of the VELO.

To protect the silicon tip from thermal effects after high irradiation, each module has an integrated cooling system using evaporative CO_2 circulating inside microchannels.

The work I have carried out on the VELO is needed to insure the safety of the detector. During the production of the VELO modules, it was discovered that the glue used to attach the VeloPix ASICs to the cooling substrate could detach, leading to a poor thermal connection to the ASIC which could overheat. The cause of the glue issue was found and fixed, but the only way to spot it if it ever happens in the install detector is to measure the temperature of the ASIC itelf.

My task has involved calibrating the temperature measured by each of the ASICs by creating a control panel through where the user can input a temperature to be used as reference for the calibration and display the raw temperature, voltage, and calibrated temperature data for each ASIC on the screen.

Once the calibration was done, we conducted experiments with the VELO at different oper-

ating powers, where we monitored the difference in temperature observed between the various power consumption mode and thereby verify the proper functioning of the subdetector.

2 Calibration

This section summarizes the reasoning and procedure followed to calibrate the temperature of each ASIC of the detector individually so that the measured temperature is as close as possible to the exact real-time temperature.

2.1 Structure per module

Each VELO pixel module consists of twelve VeloPix ASICs, each featuring a matrix of 256x256 square pixels with a size of 55 μm per side. These ASICs are grouped in sets of three, forming a tile. Four tiles are then arranged in an "L" shape around the LHCb beam pipe (see Figure 2). To ensure full coverage in the inner region, two silicon sensors are mounted on each side of the module, allowing for electrical connections to the innermost ASICs.

The cooling of the tile is supplied by a microchannel substrate onto which the tiles are glued. However, the part of the silicon sensors close to the beam axis is most vulnerable to thermal runaway.

Each module is equipped with four Negative Temperature Coefficient (NTC) thermistors, a type of resistor that exhibits a change in resistance corresponding to temperature variations. NTC thermistors, in particular, display a negative temperature coefficient, meaning their resistance decreases as temperature rises. These thermistors have been strategically positioned on the PCB alongside specific ASICs integrated into the sensor assembly, with one thermistor allocated to each of the four tiles. NTC0, located within tile 0, is in close proximity to ASIC VP1.1, while NTC2, situated within tile 2, is adjacent to ASIC VP3.1, see Figure 2. Therefore, when the cooling connection between the ASICs and the cooling plate is functioning correctly, these thermistors should register temperatures nearly identical to those of the corresponding ASICs. This similarity in temperature allows for the use of these thermistors as calibration reference points. However, in the event of a poor cooling connection, such as when the adhesive delaminates, the thermistors will not detect any temperature changes. This is precisely why we rely on the bandgap measurement as an alternative indicator in such situations.

For temperature calibration purposes, the temperature indicated by NTC2 serves as the reference temperature for each module, although it is also possible to utilize data from NTC0. Prior to calibration, it is essential to create a file for the moment when temperature data from NTC2 in each module wants to be acquired. This file is utilized in the subsequent panel, which will be explained later in the section 3, to calculate the corresponding offset for each detector ASIC. The equation to be applied is as follows:

$$b = NTC2_{temp} - 471.99\ v \tag{1}$$

Here, b represents the offset, $NTC2$ denotes the reference temperature taken for each module (shared by all 12 ASICs) and the slope is obtained from the VeloPix manual, see Figure 3.

The Bandgap circuit is used to generate a stable reference voltage for the digital-to-analog converters. The PTAT circuit is used to monitor the chip temperature since it will provide a

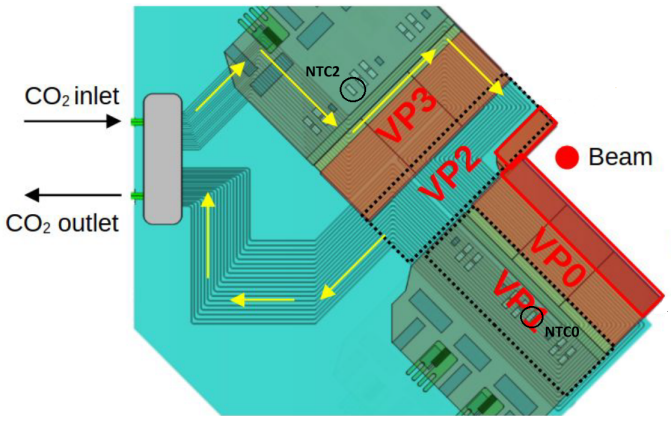

Figure 2: View of a module with two 3x1 tiles on each side. Sensors at the back (VP3 and VP0), sensors at the front (VP2 and VP1), microchannel cooling substrate (indicated by yellow arrows), ASIC bottom sides (encircled in red).

linear temperature-dependent voltage. Through the experimental measurement of the PTAT temperature and voltage a series of plots have been reconstructed which form the Figure 3, being the intermediate function (represented in green) through which I have obtained the offset equation b.

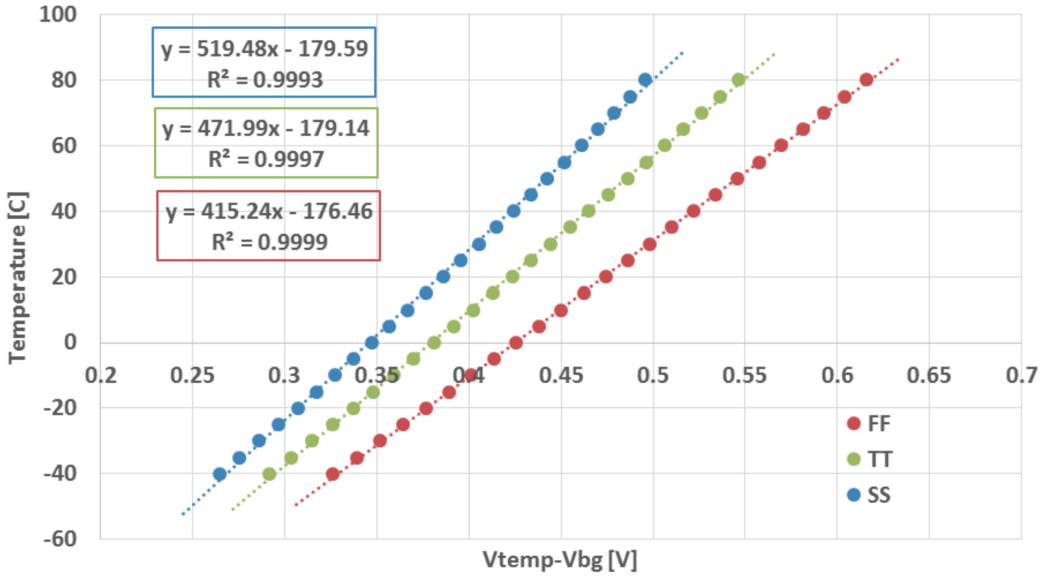

Figure 3: Simulated temperature measurement in VeloPix.

2.2 Temperature distribution

The horizontal and vertical dimensions of the substrate are 80 and 104 mm, respectively, resulting in temperature variations across its surface. Consequently, the reference temperature per

module obtained from the NTCs cannot be generalized for all 12 ASICs within that module.

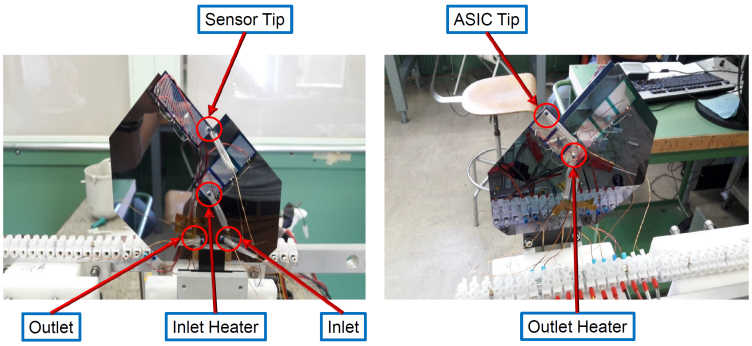

(a) Temperature probes.

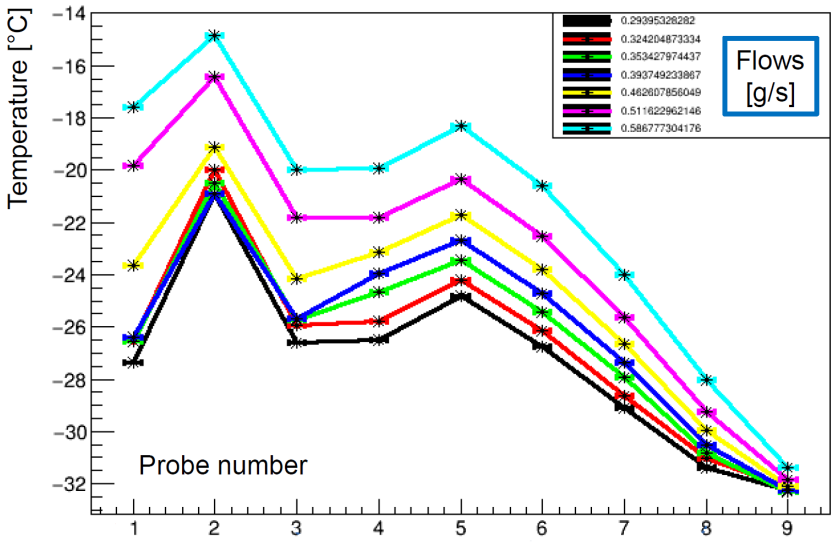

(b) Temperatures profile, load on.

Figure 4: Images obtained from reference [1].

Based on previously acquired temperature distribution data from sensors placed on the substrate, as shown in Figure 4, we have generated a temperature distribution graph under load conditions for an approximate flow rate of 0.4 g/s (dark blue line in Figure 5).

Now that we have a better understanding of the temperature variation between each ASIC and the reference temperature of NTC2, we can calculate more accurately the offset for each ASIC by slightly modifying (1). This results in the equation (2).

$$b = NTC2_{temp} + \Delta T - 471.99\ v \tag{2}$$

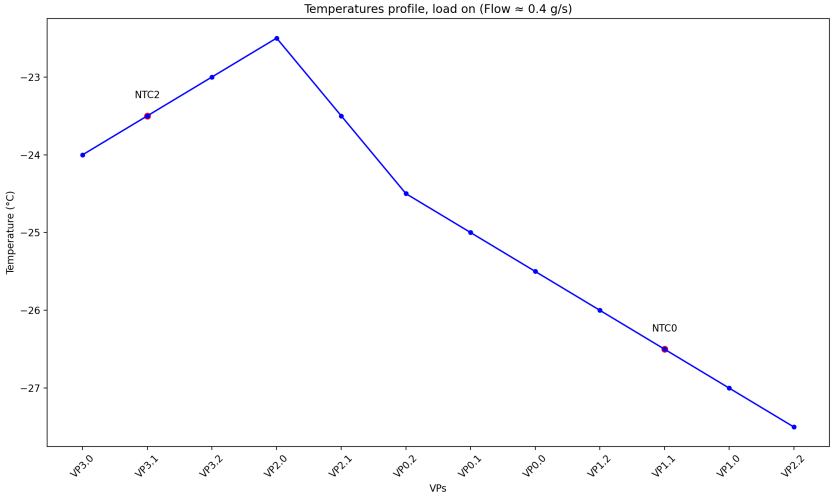

Figure 5: Temperature distribution for a nominal flow rate of 0.4 g/s.

2.3 Temperatures obtained during calibration

This section shows the temperature distribution for five of the detector modules across their surfaces. The first figure represents the raw temperature, in which we can observe a large temperature variation between the ASICs (Figure 6). The second corresponds to the temperatures calculated from a single reference temperature per module, i.e., following the equation (1) without taking into account the temperature change along the surface. A nearly constant temperature distribution is observed along the modules (Figure 7). The last plot (Figure 8) corresponds to the calibrated temperatures taking into account the temperature variation between ASICs within the same module, i.e. using the equation (2). We can see less constancy.

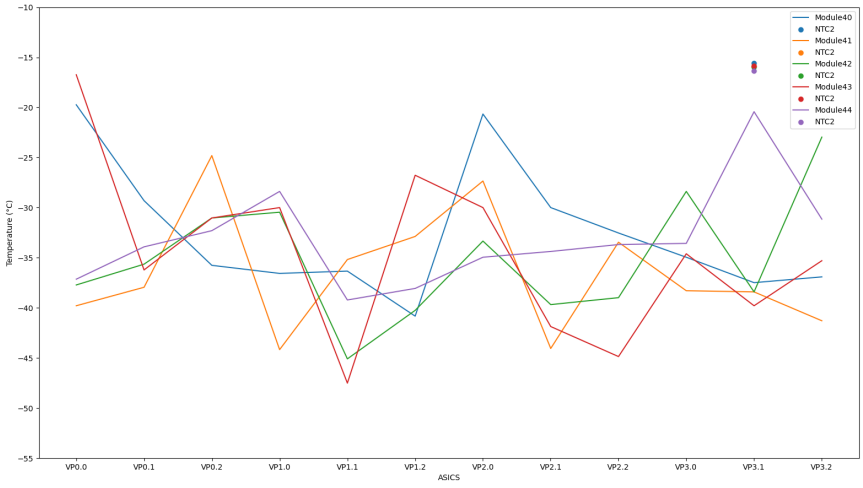

Figure 6: Uncalibrated bandgap temperature.

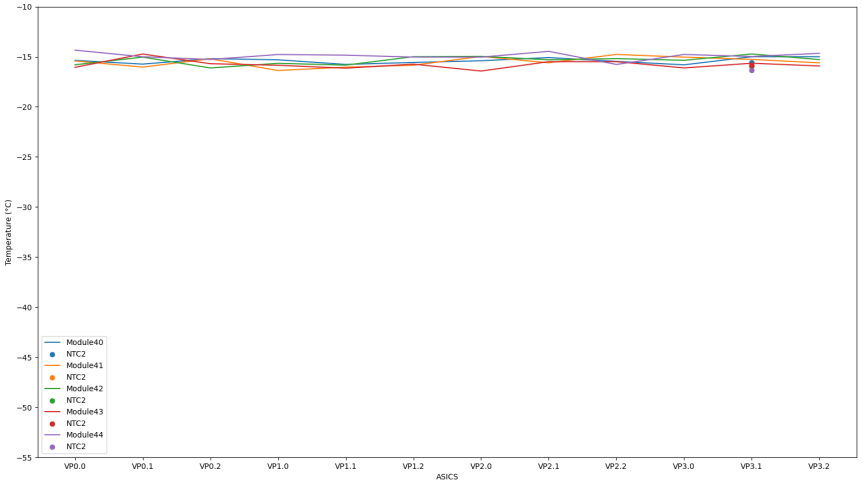

Figure 7: Bandgap temperature calibrated without the ΔT component.

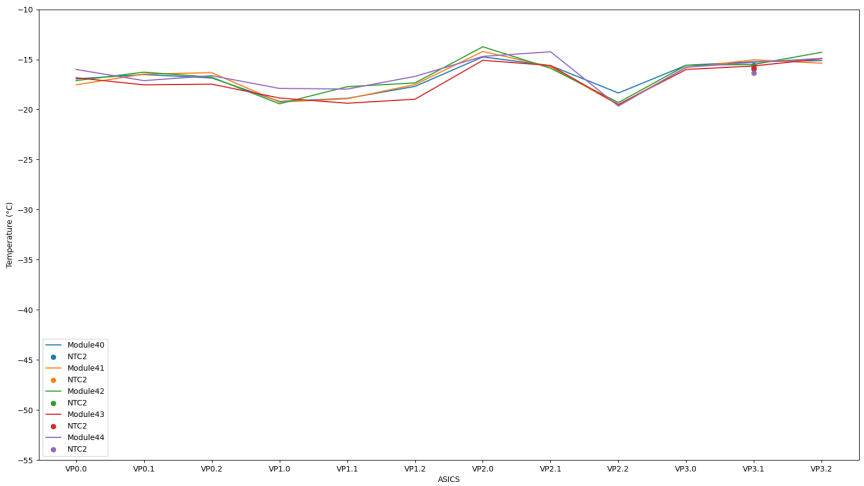

Figure 8: Bandgap temperature calibrated with the ΔT model described in Fig. 5.

3 Control panel

To provide real-time monitoring of what is happening in the detector, a panel has been developed where the data for each ASIC in the detector can be displayed. Voltage data, calibrated temperature or temperature calculated from the VeloPix manual (Bandgap Temperature or raw temperature) can be displayed.

3.1 Development tool

For project implementation, a variety of tools and programming languages were employed. The primary tool utilized for panel creation was SIMATIC WinCC Open Architecture, a system designed for centralized process monitoring and operation. Configuration of the panel was

accomplished by scripting in a language closely resembling C++. Additionally, to acquire real-time data, generate graphs, and perform result comparisons, Python was utilized as the programming language.

3.2 Structure and operation

The structure of the dashboard is divided into four tables to make the visualisation of the data more comfortable and to be able to see all the data at a glance. In the columns we have ordered the detector modules from 00 to 51, making a total of 52 columns. In the rows we have firstly a number from 0 to 3 that indicates the sensor from which the data is obtained, followed by a second number, from 0 to 2, that indicates which ASIC of the sensor data corresponds to.

To choose the type of data to be displayed in the tables, at the right of the tables there is a drop-down menu with the option of displaying the voltage, the calibrated temperature or the Bandgap temperature. To confirm the selected option, it is necessary to press the "OK" button, and the tables will display the values corresponding to the selected data type, see Figure 9.

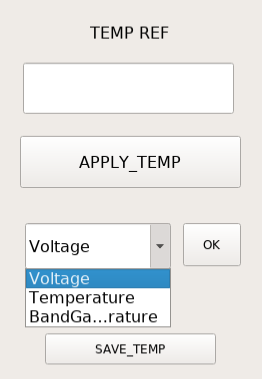

Figure 9: Control panel area.

In the upper part there is a Text Rectangle where the name of the text file containing the temperature data of the NTC2s to be used to recalibrate the temperature of each ASIC must be entered. To recalibrate it, the button $APPLY\_TEMP$ must be pressed once the file name has been entered. This calculates, following the explanations given in previous sections, and saves in another text file the offset corresponding to each ASIC of the detector. Finally, at the bottom, there is the $SAVE\_TEMP$ button which, when pressed, saves the calibrated temperature data shown in the table in another text file. It is also possible by slightly modifying the script to save the Bandgap temperature data. This last button was created with the intention of graphing and visualizing the differences between the two types of temperature data displayed in the control panel.

The appearance of the complete control panel can be seen in Figures 10a and 10b. In the first one we are showing the uncalibrated or raw temperature while in the second one the calibrated one. We see clear contrasts between the two figures. While in 10a there are large differences (as significant as 20 ^oC or even more) between the temperatures of different ASICs, these discrepancies are reduced to approximately 4 ^oC in the calibrated temperature values of 10b, bringing them closer to the expected operating temperature.

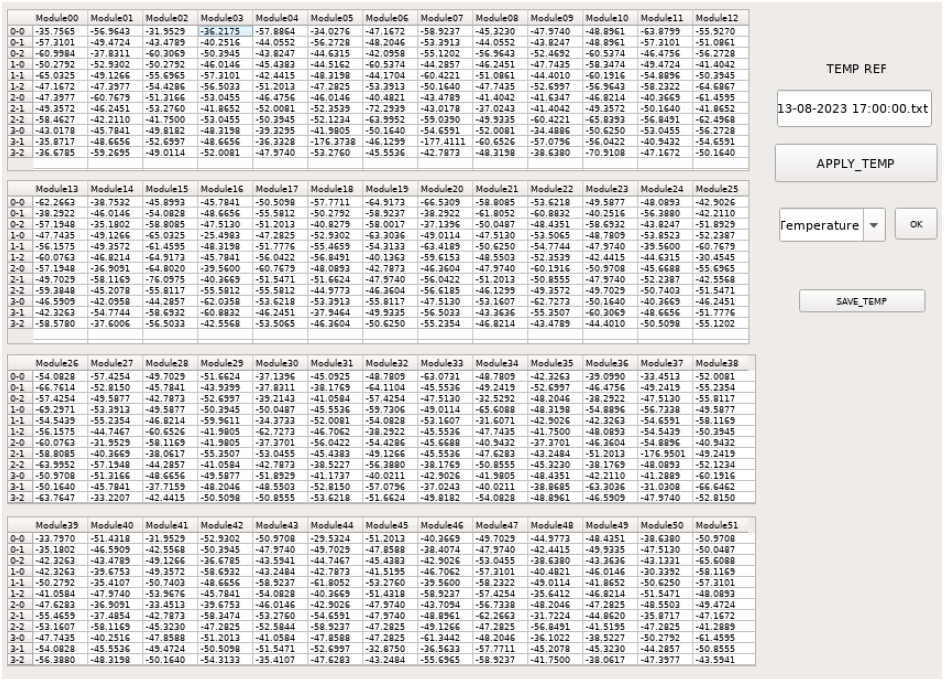

	Module00	Module01	Module02	Module03	Module04	Module05	Module06	Module07	Module08	Module09	Module10	Module11	Module12
0-0	-35.7565	-56.9642	-31.9529	-36.2175	-57.8864	-34.0276	-47.1672	-58.9237	-45.3230	-47.9740	-48.8961	-63.8799	-55.9270
0-1	-57.3101	-49.4724	-42.4789	-40.2516	-44.0552	-56.2729	-48.2046	-53.3913	-44.0552	-43.8247	-48.8961	-57.3101	-51.0861
0-2	-60.9984	-37.8311	-60.3069	-50.3945	-43.8247	-44.6315	-42.0958	-55.1202	-56.9643	-52.4692	-60.5374	-46.4756	-56.2728
1-0	-50.2792	-52.9302	-50.2792	-46.0146	-45.4383	-44.5162	-60.5374	-44.2857	-46.2451	-47.7435	-58.3474	-49.4724	-41.4042
1-1	-65.0325	-49.1266	-55.6965	-57.3101	-42.4415	-48.3198	-44.1704	-60.4221	-51.0861	-44.4010	-60.1916	-54.8896	-50.3945
1-2	-47.1672	-47.3977	-54.4286	-56.5033	-51.2013	-47.2825	-53.3913	-50.1640	-47.7435	-52.6997	-56.9643	-58.2322	-64.6867
2-0	-47.3977	-60.7679	-51.3166	-52.0455	-46.4756	-46.0146	-40.4821	-43.4789	-41.4042	-41.6347	-46.8214	-40.3669	-61.4595
2-1	-49.3572	-46.2451	-53.2760	-41.8652	-52.0081	-52.3539	-72.2939	-43.0178	-37.0243	-41.4042	-49.3572	-50.1640	-41.8652
2-2	-58.4627	-42.2110	-41.7500	-53.0455	-50.3945	-52.1234	-63.9952	-59.0390	-49.9335	-60.4221	-65.8393	-56.8491	-62.4968
3-0	-43.0178	-45.7841	-49.8182	-48.3198	-39.3295	-41.9805	-50.1640	-54.6591	-52.0081	-34.4886	-50.6250	-53.0455	-56.2728
3-1	-35.8717	-48.6656	-52.6997	-48.6656	-36.3328	-176.3738	-46.1299	-177.4111	-60.6526	-57.0796	-56.0422	-40.9432	-54.6591
3-2	-36.6785	-59.2695	-49.0114	-52.0081	-47.9740	-53.2760	-45.5536	-42.7873	-48.3198	-38.6380	-70.9108	-47.1672	-50.1640

	Module13	Module14	Module15	Module16	Module17	Module18	Module19	Module20	Module21	Module22	Module23	Module24	Module25
0-0	-62.2663	-38.7532	-45.8993	-45.7841	-50.5098	-57.7711	-64.9173	-66.5309	-58.8085	-53.6218	-49.5877	-48.0893	-42.9026
0-1	-38.2922	-46.0146	-54.0828	-48.6656	-55.5812	-50.2792	-58.9237	-38.2922	-61.8052	-60.8832	-40.2516	-56.3880	-42.2110
0-2	-57.1948	-35.1802	-58.8085	-47.5130	-51.2013	-40.8279	-58.0017	-37.1396	-50.0587	-48.4351	-58.6932	-43.8247	-51.8929
1-0	-47.7435	-49.1266	-65.0325	-25.4983	-47.2825	-52.9302	-63.3036	-49.0114	-47.5130	-53.5065	-48.7809	-53.8523	-52.2387
1-1	-56.1575	-49.3572	-61.4595	-48.3198	-51.7776	-55.4659	-54.3133	-63.4189	-50.6250	-54.7744	-47.9740	-39.5600	-60.7679
1-2	-60.0763	-46.8214	-64.9173	-45.7841	-56.0422	-56.8491	-40.1363	-59.6153	-48.5503	-52.3539	-42.4415	-44.6315	-30.4545
2-0	-57.1948	-36.9091	-64.8020	-39.5600	-60.7679	-48.0893	-42.7873	-46.3604	-47.9740	-60.1916	-50.9708	-45.6688	-55.6965
2-1	-49.7029	-58.1169	-76.0975	-40.3669	-51.5471	-51.6624	-47.9740	-56.0422	-51.2013	-50.8555	-47.9740	-52.3287	-42.5568
2-2	-59.3848	-45.2078	-55.8117	-55.5812	-55.5812	-44.9773	-46.3604	-56.6185	-46.1299	-49.3572	-49.7029	-50.7403	-51.5471
3-0	-46.5909	-42.0958	-44.2857	-62.0358	-53.6218	-53.3913	-55.8117	-47.5130	-53.1607	-62.7273	-50.1640	-40.3669	-46.2451
3-1	-42.3263	-54.7744	-58.6932	-60.8832	-46.2451	-37.9464	-49.9335	-56.5033	-43.3636	-55.3507	-60.3069	-48.6656	-51.7776
3-2	-58.5780	-37.6006	-56.5033	-42.5568	-53.5065	-46.3604	-50.6250	-55.2354	-46.8214	-43.4789	-44.4010	-50.5098	-55.1202

	Module26	Module27	Module28	Module29	Module30	Module31	Module32	Module33	Module34	Module35	Module36	Module37	Module38
0-0	-54.0828	-57.4254	-49.7029	-51.6624	-37.1396	-45.0925	-48.7809	-63.0731	-48.7809	-42.3263	-39.0990	-33.4513	-52.0081
0-1	-66.7614	-52.8150	-45.7841	-43.9399	-37.8311	-38.1769	-64.1104	-45.5536	-49.2419	-52.6997	-46.4756	-49.2419	-55.2354
0-2	-57.4254	-49.5877	-42.7873	-52.6997	-39.2143	-41.0584	-57.4254	-47.5130	-32.5292	-48.2046	-38.2922	-47.5130	-55.8117
1-0	-69.2971	-53.3913	-49.5877	-50.3945	-50.0487	-45.5536	-59.7306	-49.0114	-65.6088	-48.3198	-54.8896	-56.7338	-49.5877
1-1	-54.5439	-55.2254	-46.8214	-59.9611	-24.3733	-52.0081	-54.0828	-53.1607	-31.6071	-42.9026	-42.2263	-54.6591	-58.1169
1-2	-56.1575	-44.7467	-60.6526	-41.9805	-62.7273	-46.7062	-38.2922	-45.5536	-47.7435	-41.7500	-48.0893	-54.5439	-50.3945
2-0	-60.0763	-31.9529	-58.1169	-41.9805	-37.3701	-56.0422	-54.4286	-45.6688	-40.9432	-37.3701	-46.3604	-54.8896	-40.9432
2-1	-58.8085	-40.3669	-38.0617	-55.3507	-53.0455	-45.4383	-49.1266	-45.5536	-47.6283	-43.2484	-51.2013	-176.9501	-49.2419
2-2	-63.9952	-57.1948	-44.2857	-41.0584	-42.7873	-38.5227	-56.3880	-38.1769	-50.8555	-45.3230	-38.1769	-48.0893	-52.1234
3-0	-50.5708	-51.3166	-48.6656	-49.5877	-51.8929	-41.1737	-40.0211	-42.9026	-41.9805	-48.4351	-42.2110	-41.2889	-60.1916
3-1	-50.1640	-45.7841	-37.7159	-48.2046	-48.5503	-52.8150	-57.0796	-37.0243	-40.0211	-38.8685	-63.3036	-31.0308	-66.6462
3-2	-63.7647	-33.2207	-42.4415	-50.5098	-50.8555	-53.6218	-51.6624	-49.8182	-54.0828	-48.8961	-46.5909	-47.9740	-52.8150

	Module39	Module40	Module41	Module42	Module43	Module44	Module45	Module46	Module47	Module48	Module49	Module50	Module51
0-0	-33.7970	-51.4318	-31.9529	-52.9302	-50.9708	-29.5324	-51.2013	-40.3669	-49.7029	-44.9773	-48.4351	-38.6380	-50.9708
0-1	-35.1802	-46.5909	-42.5568	-50.3945	-47.9740	-49.7029	-47.8588	-38.4074	-47.9740	-42.4415	-49.9335	-47.5130	-50.0487
0-2	-42.3263	-42.4789	-49.1266	-36.5748	-43.5941	-44.7467	-45.4383	-49.9026	-53.0455	-28.6380	-43.3636	-43.1231	-65.6088
1-0	-42.3263	-39.6753	-49.3572	-58.6932	-43.2484	-42.7873	-41.5195	-46.7062	-57.3101	-40.4821	-46.0146	-20.3392	-58.1169
1-1	-50.2792	-35.4107	-50.7403	-48.6656	-58.9237	-61.8052	-53.2760	-39.5600	-58.2322	-49.0114	-41.8652	-50.6250	-57.3101
1-2	-41.0584	-47.9740	-53.9676	-45.7841	-54.0828	-40.3669	-51.4318	-58.9237	-57.4254	-35.6412	-46.8214	-51.5471	-48.0893
2-0	-47.6283	-36.9091	-33.4513	-39.6753	-46.0146	-42.9026	-47.9740	-43.7094	-56.7338	-48.2046	-47.2825	-48.5503	-49.4724
2-1	-55.4659	-27.4854	-42.7873	-58.3474	-53.2760	-54.6591	-47.9740	-48.8961	-62.2663	-31.7224	-44.8620	-35.8717	-47.1672
2-2	-53.1607	-58.1169	-45.3230	-47.2825	-52.5844	-58.9237	-47.2825	-49.1266	-47.2825	-56.8491	-41.5195	-47.2825	-41.2889
3-0	-47.7435	-40.2516	-47.8588	-51.2013	-41.0584	-47.8588	-47.2825	-61.3442	-48.2046	-36.1022	-38.5227	-50.2792	-61.4595
3-1	-54.0828	-45.5536	-49.4724	-50.5098	-51.5471	-52.6997	-32.8750	-36.5633	-57.7711	-45.2078	-45.3230	-44.2857	-50.8555
3-2	-56.3880	-48.3198	-50.1640	-54.3133	-35.4107	-47.6283	-43.2484	-55.6965	-58.9237	-41.7500	-38.0617	-47.3977	-43.5941

(a) Bandgap Temperatures.

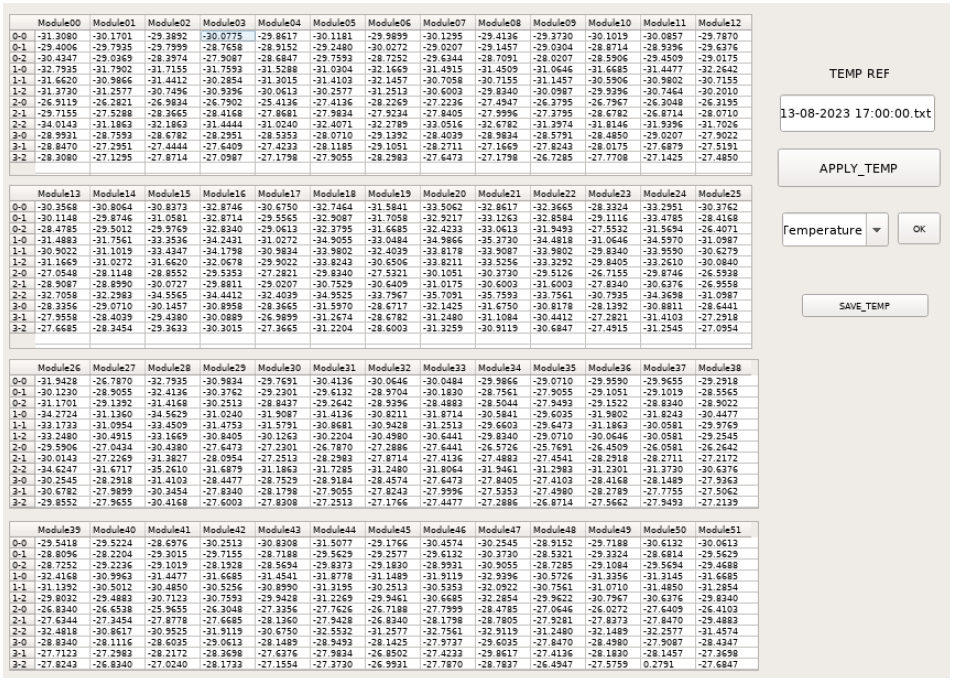

	Module00	Module01	Module02	Module03	Module04	Module05	Module06	Module07	Module08	Module09	Module10	Module11	Module12
0-0	-31.3080	-30.1701	-29.3892	-30.0775	-29.8617	-30.1181	-29.9899	-30.1295	-29.4136	-29.3730	-30.1019	-30.0857	-29.7870
0-1	-29.4006	-29.7935	-29.7999	-28.7658	-28.9152	-29.2480	-30.0272	-29.0207	-29.1457	-29.0304	-28.8714	-28.9336	-29.6376
0-2	-30.4347	-29.0269	-28.3974	-27.9087	-28.6847	-29.7593	-28.7252	-29.6344	-28.7091	-28.0207	-28.5906	-29.4509	-29.0175
1-0	-32.7935	-31.7902	-31.7155	-31.7593	-31.5288	-31.0304	-32.1669	-31.4915	-31.4509	-31.0646	-31.6685	-31.4477	-32.2642
1-1	-31.6620	-30.9866	-31.4412	-30.2854	-31.3015	-31.4103	-32.1457	-30.7058	-30.7155	-31.1457	-30.5906	-30.9802	-30.7155
1-2	-31.3730	-31.2577	-30.7496	-30.9396	-30.0613	-30.2577	-31.2513	-30.6003	-29.8340	-30.0987	-29.9396	-30.7464	-30.2010
2-0	-26.9119	-26.2821	-26.9834	-26.7902	-25.4136	-27.4136	-28.2269	-27.2236	-27.4947	-26.3795	-26.7967	-26.3048	-26.3195
2-1	-29.7155	-27.5288	-28.4168	-28.4168	-27.8681	-27.9834	-27.9234	-27.8405	-27.9996	-27.3795	-28.6782	-26.8714	-28.0710
2-2	-34.0143	-31.1863	-32.1863	-31.4444	-31.0240	-32.4071	-32.2789	-33.0516	-32.6782	-31.3974	-31.8146	-31.9396	-31.7026
3-0	-28.9931	-28.7593	-28.6782	-28.2951	-28.5353	-28.0710	-29.1392	-28.4039	-28.9834	-28.5791	-28.4850	-29.0207	-27.9022
3-1	-28.8470	-27.2951	-27.4444	-27.6409	-27.4233	-28.1185	-29.1051	-28.2711	-27.1669	-27.8243	-28.0175	-27.6879	-27.5191
3-2	-28.3080	-27.1295	-27.8714	-27.0987	-27.1798	-27.9055	-28.2983	-27.6473	-27.1798	-26.7285	-27.7708	-27.1425	-27.4850

	Module13	Module14	Module15	Module16	Module17	Module18	Module19	Module20	Module21	Module22	Module23	Module24	Module25
0-0	-30.3568	-30.8064	-30.8373	-32.8746	-30.6750	-32.7464	-31.5841	-33.5062	-32.8617	-32.3665	-28.3324	-33.2951	-30.3762
0-1	-30.1148	-29.8746	-31.0581	-32.8714	-29.5565	-32.9087	-31.7058	-32.9217	-33.1263	-32.8584	-29.1116	-33.4785	-28.4168
0-2	-28.4785	-29.5012	-29.9769	-32.8340	-29.0613	-32.3795	-31.6685	-32.4233	-33.0613	-31.9493	-27.5532	-31.5694	-26.4071
1-0	-31.4883	-31.7561	-33.2536	-34.4412	-31.0272	-34.9055	-33.0484	-34.9866	-35.3730	-34.4818	-31.0646	-34.5970	-31.0987
1-1	-30.9022	-31.1019	-33.4347	-34.1798	-30.9834	-33.9802	-32.4039	-33.8178	-33.9087	-33.9802	-29.8340	-33.9550	-30.6279
1-2	-31.1669	-31.0272	-31.6620	-32.0678	-29.9022	-33.8243	-30.6506	-33.8211	-33.5256	-33.3292	-29.8405	-33.2610	-30.0840
2-0	-27.0548	-28.1148	-28.8552	-29.5353	-27.2821	-29.8340	-27.5321	-30.1051	-30.3730	-29.5126	-26.7155	-29.8746	-26.5938
2-1	-28.9087	-28.8990	-30.0727	-29.8811	-29.0207	-30.7529	-30.6409	-31.0175	-30.6003	-31.6003	-27.8340	-30.6376	-26.9558
2-2	-32.7058	-32.2983	-34.5565	-34.4412	-32.4039	-34.9525	-32.7967	-35.7091	-35.7593	-31.7561	-30.7935	-34.3698	-31.0987
3-0	-28.3356	-29.0710	-30.1457	-30.8958	-28.3665	-31.5970	-28.6717	-32.1425	-31.6750	-30.8178	-28.1392	-30.8811	-28.6441
3-1	-27.9558	-28.4039	-29.4380	-30.0889	-26.9899	-31.2674	-28.6782	-31.2480	-31.1084	-30.4412	-27.2821	-31.4103	-27.2918
3-2	-27.6685	-28.3454	-29.3633	-30.3015	-27.3665	-31.2204	-28.6003	-31.3259	-30.9119	-30.6847	-27.4915	-31.2545	-27.0954

	Module26	Module27	Module28	Module29	Module30	Module31	Module32	Module33	Module34	Module35	Module36	Module37	Module38
0-0	-31.9428	-26.7870	-32.7935	-30.9834	-29.7691	-30.4136	-30.0646	-30.0484	-29.9866	-29.0710	-29.9550	-29.9655	-29.2918
0-1	-30.1230	-28.9055	-32.4136	-30.3762	-29.2301	-29.6132	-28.9704	-30.1830	-28.7561	-27.9055	-29.1051	-29.1019	-28.5565
0-2	-31.1701	-29.1392	-31.4168	-30.2513	-28.8437	-29.2642	-28.9396	-28.4883	-28.5044	-27.9493	-29.1522	-28.8340	-28.9022
1-0	-34.2724	-31.1360	-34.5629	-31.0240	-31.9087	-31.4136	-30.8211	-31.8714	-30.5841	-29.6035	-31.9802	-31.8243	-30.4477
1-1	-33.1733	-31.0954	-33.4509	-31.4753	-31.5791	-30.8681	-30.9428	-31.2513	-29.6603	-29.6473	-31.1863	-30.0581	-29.9769
1-2	-32.2480	-30.4915	-32.1669	-30.8405	-30.1263	-30.2204	-30.4980	-30.6441	-29.8340	-29.0710	-30.0646	-30.0581	-29.2545
2-0	-29.5906	-27.0434	-30.4380	-27.6473	-27.2301	-26.7870	-27.2886	-27.6441	-26.5726	-25.7691	-26.4509	-26.0581	-26.2642
2-1	-30.0143	-27.2269	-31.3827	-28.0954	-27.2513	-28.2983	-27.8714	-27.4136	-27.4883	-27.4541	-28.2918	-28.2711	-27.2172
2-2	-34.6247	-31.6717	-35.2610	-31.6879	-31.1863	-31.7285	-31.2480	-31.8064	-31.9461	-31.2983	-31.2301	-31.3730	-30.6376
3-0	-30.2545	-28.2918	-31.4103	-28.4477	-28.7529	-28.9184	-28.4574	-27.6473	-27.8405	-27.4103	-28.4168	-28.1489	-27.9363
3-1	-30.6782	-27.9899	-30.3454	-27.8340	-28.1798	-27.9055	-27.8243	-27.9996	-27.5353	-27.4980	-28.2789	-27.7755	-27.5062
3-2	-29.8552	-27.9655	-30.4168	-27.6003	-27.8308	-27.2513	-27.1766	-27.4477	-27.2886	-26.8714	-27.5662	-27.9492	-27.2139

	Module39	Module40	Module41	Module42	Module43	Module44	Module45	Module46	Module47	Module48	Module49	Module50	Module51
0-0	-29.5418	-29.5224	-28.6976	-30.2513	-30.8308	-31.5077	-29.1766	-30.4574	-30.2545	-28.9152	-29.7188	-30.6132	-30.0613
0-1	-28.8096	-28.2204	-29.3015	-29.7155	-28.7188	-29.5629	-29.2577	-29.6132	-30.3730	-28.5321	-29.3324	-28.6814	-29.5629
0-2	-28.7252	-29.2236	-29.1019	-28.1523	-28.5694	-29.8373	-29.1830	-28.9931	-30.9055	-28.7285	-29.1084	-29.5694	-29.4688
1-0	-32.4168	-30.9963	-31.4477	-31.6685	-31.4541	-31.8778	-31.1489	-31.9119	-32.9396	-30.5726	-31.2356	-31.2145	-31.6685
1-1	-31.1392	-30.5012	-30.4850	-30.5256	-30.8990	-31.3195	-30.2513	-30.5353	-32.0922	-30.7561	-31.0710	-31.4850	-31.2854
1-2	-29.8032	-29.4883	-30.7123	-30.7593	-29.9428	-31.2269	-29.9461	-30.6685	-32.2854	-29.9622	-30.7967	-30.6376	-29.8340
2-0	-26.8340	-26.6538	-25.9655	-26.3048	-27.3356	-27.7626	-26.7188	-27.7999	-28.4785	-27.0646	-26.0272	-27.6409	-26.4103
2-1	-27.6344	-27.3454	-27.8778	-27.6685	-28.1360	-27.9428	-26.8340	-28.1798	-28.7805	-27.9291	-27.8373	-27.8470	-29.4883
2-2	-32.4818	-30.8617	-30.9525	-31.9119	-30.6750	-32.5532	-31.2577	-32.7561	-32.9119	-31.2480	-32.1489	-32.2577	-31.4574
3-0	-28.8340	-28.1116	-28.6035	-29.0613	-28.1489	-28.9493	-28.1425	-27.9737	-29.6035	-27.8470	-28.4980	-27.9087	-28.4347
3-1	-27.7123	-27.2983	-28.2172	-28.3698	-27.6376	-27.9824	-26.8502	-27.4233	-29.8617	-27.4136	-28.1830	-28.1457	-27.3698
3-2	-27.8243	-26.8340	-27.0240	-28.1733	-27.1554	-27.3730	-26.9931	-27.7870	-28.7837	-26.4947	-27.5759	0.2791	-27.6847

(b) Calibrated temperatures.

Figure 10: Real-time data control panel displaying calibrated and non calibrated temperature data

4 Cross-checking of production measurements

The quality of the adhesive layer beneath the tiles is related to the temperature behavior as a function of power. To verify this behavior by obtaining calibrated temperature data at approximately 12 W and 23 W, we can calculate the maximum absolute temperature variation for each sensor in each module (Figure 11). We can see that the measurements of temperature in absolute value obtained in the table are correct, maximum about 4 ^oC, which means that the glue problem no longer exists for a long time due to correction during production. If the detector is not in operation, we could use this method to compare the production side graphs.

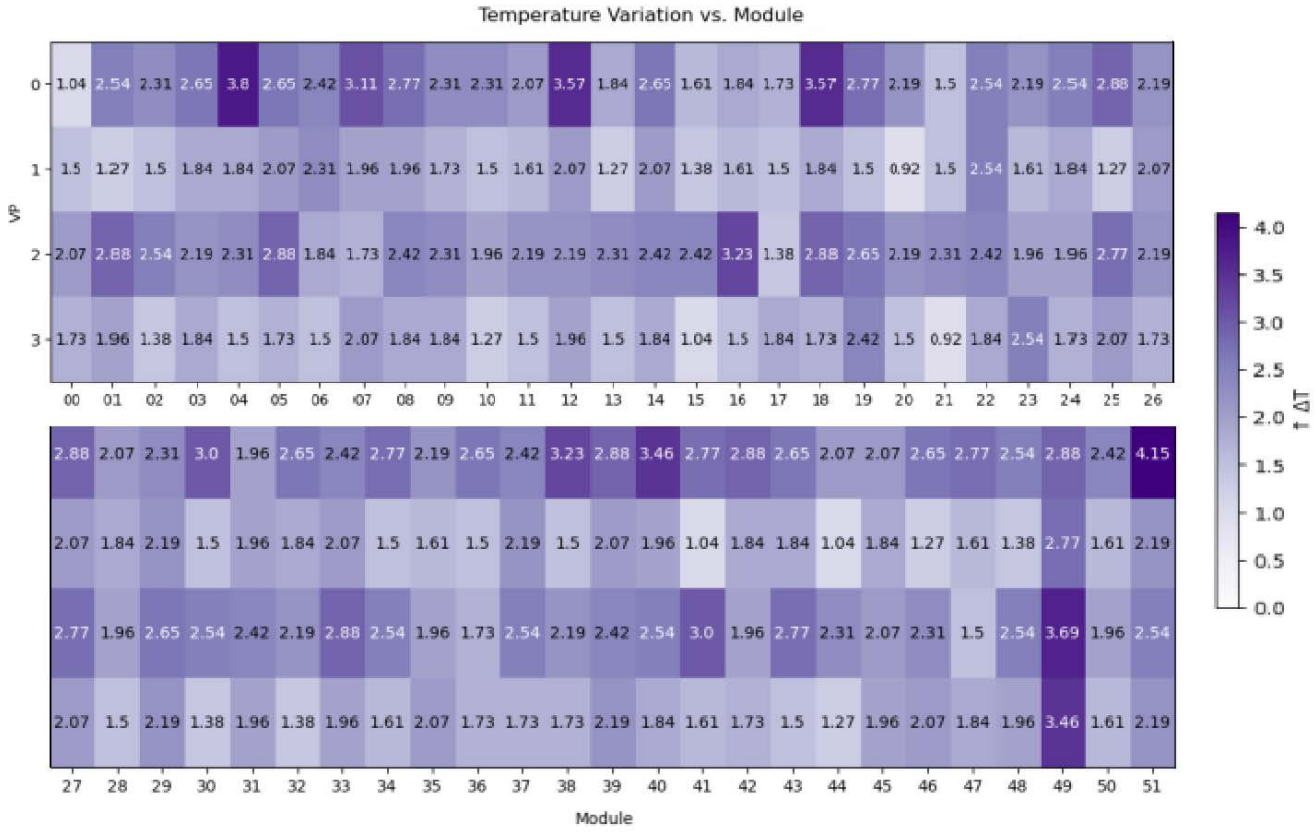

Figure 11: Power vs Temperature.

5 Conclusion

In this report, I have focused on developing a calibration method for temperature measurement of individual ASICs within the VErtex LOcator (VELO), a vital subdetector of the LHCb experiment at CERN. The aim was to address anomalies observed in previous temperature measurements of the ASICs and ensure the VELO's dependable performance under varying power conditions.

Using the WinCC Open Architecture tool, we successfully designed a control panel that offers real-time display of calibrated temperature data for each ASIC, alongside other temperature and voltage readings.

Additionally, we conducted experiments with the VELO at various power levels, collecting temperature data from the ASICs. We calculated the absolute differences between these temperatures, serving as a crucial indicator of the VELO's proper functioning.

In summary, the successful implementation of the temperature measurement calibration method within the VELO, coupled with the development of the control panel, has contributed to improved data quality and experiment control.

References

[1] Wiktor Byczyński, *R&D on CO_2 cooling using a silicon microchannel substrate for the LHCb VELO*, Forum on Tracking Detector Mechanics, Valencia (2018).

[2] The LHCb Collaboration, *LHCb VELO Upgrade Technical Design Report*, CERN LHCb, (2013).

[3] Xavier Llopart and Tuomas Poikela, *VeloPix Operation Manual*, CERN LHCb, (2023).

[4] Peter Svihra, *The Design and Construction of LHCb VELO Upgrade Modules*, CERN LHCb, (2020).

[5] Daniel Hynds, *Why are we here?*, VELO module production meeting, CERN LHCb, (2020).